

---

## Research Submission

---

# Resting State Functional Connectivity After Sphenopalatine Ganglion Blocks in Chronic Migraine With Medication Overuse Headache: A Pilot Longitudinal fMRI Study

Kaitlin Krebs, MSc; Chris Rorden, PhD; X. Michelle Androulakis, MD, MSc

**Objective.**—In this pilot study, the purpose is to investigate if a series of sphenopalatine ganglion (SPG) blockade treatments modulate the functional connectivity within the salience and central executive network (CEN) in chronic migraine with medication overuse headaches (CM<sup>w/MOH</sup>).

**Background.**—Using intranasal local anesthesia to block the SPG for the treatment of various headache disorders has been employed in clinical practice since the early 1900s. However, the exact mechanism of how SPG modulate resting state intrinsic functional brain networks connectivity remains to be elucidated. This pilot study seeks to understand the resting state connectivity changes in salience and CENs, with emphasis on the mesocorticolimbic systems, before and after a series of SPG block treatments.

**Methods.**—Using fMRI, resting state connectivity was derived from predefined networks of nodes (regions of interests) for the salience (27 nodes, 351 connections) and CENs (17 nodes, 136 connections). After treatments, a paired samples *t*-test (with 10,000 permutations to correct for multiple comparison) was used to evaluate changes in the intranetwork resting state functional connectivity within the salience and executive networks, as well as the overall network connectivity strength.

**Results.**—When comparing connectivity strength at baseline to that at the end of treatment in our cohort of 10 CM<sup>w/MOH</sup> participants, there were several connections within the salience (*n* = 9) and executive (*n* = 8) networks that were significantly improved. Within the salience network, improved connectivity was observed between the prefrontal cortex and various regions of the insula, basal ganglia, motor, and frontal cortex. Additionally, changes in connectivity were observed between regions of the temporal cortex with the basal ganglia and supramarginal gyrus. Within the CEN, improved connectivity was observed between the prefrontal cortex and regions of the anterior thalamus, caudate, and frontal cortex. After treatment, the overall CEN connectivity was significantly improved (Baseline  $0.00 \pm 0.08$ ; 6 weeks  $0.03 \pm 0.09$ ,  $P = .01$ ); however, the overall salience network connectivity was not significantly improved (Baseline  $-0.01 \pm 0.10$ ; 6 weeks  $0.01 \pm 0.12$ ,  $P = .26$ ). Additionally, after treatment, there was a significant reduction in the number of moderate/severe headache days per month (Baseline  $21.1 \pm 6.6$ ; 6 weeks  $11.2 \pm 6.5$ ,  $P < .001$ ), HIT-6 (Baseline  $66.1 \pm 2.6$ ; 6 weeks  $60.2 \pm 3.6$ ,  $P < .001$ ), and PHQ-9 (Baseline  $12.4 \pm 5.7$ ; 6 weeks  $6.1 \pm 3.6$ ,  $P = .008$ ) scores.

**Conclusion.**—In this longitudinal fMRI study, we observed improved functional connectivity within both networks, primarily involving connectivity between regions of the prefrontal cortex and limbic (cortical-limbic) structures, and between different cortical (cortical-cortical) regions after a series of repetitive SPG blockades. The overall CEN strength was also

---

From the School of Medicine, Department of Neurology, University of South Carolina, Columbia, SC, USA.

Address all correspondence to X.M. Androulakis, University of South Carolina School of Medicine, Department of Neurology, Columbia, SC 29203.

Accepted for publication March 11, 2018.

improved. Our results suggest that recurrent parasympathetic inhibition via SPG is associated with improved functional connectivity in brain regions critical to pain processing in CM<sup>w/MOH</sup>.

**Key words:** salience network, central executive network, fMRI, chronic migraine, sphenopalatine ganglion, resting state connectivity

**Abbreviations:** ASC 12 allodynia symptom checklist, aPFC anterior PFC, BOLD blood oxygenation level dependent, CEN central executive network, CM chronic migraine, CMw/MOH chronic migraine with medication overuse headaches, dACC dorsal anterior cingulate cortex, dCaudate dorsal caudate, dmPFC dorsal medial PFC, dPFC/FEF dorsal PFC/frontal eye field, dlPFC dorsolateral prefrontal cortex, TE echo time, EA extended amygdala, FOV field of view, HIT-6 headache impact test, IFG inferior frontal gyrus, MP-RAGE magnetization-prepared rapid gradient echo, MNI Montreal Neurological Institute, NTNC node to node connectivity, NSAIDs nonsteroidal anti-inflammatory drugs, OFI orbitofrontal insula, PHQ-9 Patient Health Questionnaire, PAG periaqueductal gray, PFC prefrontal cortex, ROIs region of interest, TR repetition time, SN salience network, SPG sphenopalatine ganglion, SSN superior salivatory nucleus, SMA supplementary motor area, SMG supramarginal gyrus, vSP ventral striatum/pallidum, VTA/SNCP ventral tegmental area/Substantia nigra, vlPFC ventrolateral PFC, vmCaudate ventromedial caudate

(Headache 2018;58:732-743)

## INTRODUCTION

Sphenopalatine ganglion (SPG) plays a crucial role in migraine pathogenesis through activation of the trigemino-autonomic reflex.<sup>1,2</sup> Parasympathetic nerves arise from superior salivatory nucleus (SSN) synapses on the SPG, where postsynaptic afferents from the SPG then trigger vasodilatation of the cranial and meningeal vasculature, subsequently leading to a cascade of neuroinflammatory events that initiate migraine pain and associated autonomic symptoms.<sup>3</sup> Via its connection with the SSN, SPG has indirect link with the limbic systems and cortical regions, which are often affected in migraine populations.<sup>3-5</sup> Intranasal application of local anesthesia to the SPG is efficacious for acute pain relief, improving migraine related disability at 6 weeks post treatment.<sup>6,7</sup> The exact mechanism of SPG neuromodulation remains to be elucidated. Decreased parasympathetic outflow from the SPG block, especially in the frontal regions of the brain, is likely crucial for improved migraine pain and related symptoms.<sup>8</sup>

Our lab conducted a recent study that revealed decreased overall functional connectivity in default

*Conflict of Interest:* Kaitlin Krebs and Chris Rorden do not report any conflicts of Interest. Michelle Androulakis discloses that she was previously funded in a grant sponsored by Tian Medical.

*Funding Source:* McCausland Center for Brain Imaging (M-Fund) and University of South Carolina internal grant (ASPIRE II).

mode network, salience network (SN) and central executive network (CEN) in chronic migraine (CM) with medication overuse headache (CM<sup>w/MOH</sup>).<sup>9</sup> Further investigation of the node to node connectivity (NTNC) within the SN showed much more extensive disruption in regions involved in the mesocorticolimbic pathways bilaterally in CM<sup>w/MOH</sup> as compared to CM without MOH.<sup>10</sup> This is similar to the findings of aberrant mesocorticolimbic activity in CM<sup>w/MOH</sup> using task-based fMRI.<sup>11</sup> The mesocorticolimbic system is rich in dopaminergic neurons and serves as neural substrate for pain, addiction, reward, and goal directed behavior. Disruption in this system has been linked to both migraine and overuse of pain medications.<sup>12-14</sup>

Given that that mesocorticolimbic system plays a large role in both the SN and CEN, it is plausible that exploration into these networks may prove useful in monitoring therapeutic outcome in this population. In theory, this method may not only be used as a biomarker, but also may provide insight into the mechanisms of SPG treatment. In this pilot study, we hypothesized that repetitive parasympathetic inhibition via a series of SPG block would modulate resting state NTNC within the SN and CEN, and that such neuromodulatory effect would involve mostly mesocorticolimbic regions in CM<sup>w/MOH</sup>.

## MATERIALS AND METHODS

**Participants.**—Women were eligible for the study if they were at least 18 years old, met diagnostic

criteria fulfilling International Classification of Headache Disorders-III (beta)<sup>15</sup> for CM<sup>w/MOH</sup>, had predominantly frontal and/or orbital pain, and were eligible for receiving SPG blockade per manufacturer's instruction. Participants were excluded if they had cervicogenic headaches, or other headache treatment procedures such as nerve blocks or onabotulinumtoxinA (Botox), physical therapy, or acupuncture six months before or during the treatment period. Furthermore, participants were excluded if they had MRI contraindication, neurological or pain disorders other than CM<sup>w/MOH</sup>, any chronic illness (ie, hypertension, diabetes, hepatic, renal, chronic inflammatory, or infectious disease, etc), unable to complete all SPG treatments within 6 weeks, or inability to follow study protocol while completing assessments. To minimize any effect on functional BOLD (blood oxygenation level dependent) signal changes, participants with any possible confounding factors (ie, recreational drug use) were excluded.

All CM<sup>w/MOH</sup> participants were instructed to continue with the prophylactic medications, and use of acute pain medication as needed as usual with no new medications or headache related treatment started, throughout this 6 week period. All CM<sup>w/MOH</sup> participants were age ( $\pm 5$  years) and gender matched to healthy controls. Healthy controls were selected from a pool of healthy controls collected in a previous study.<sup>9,10</sup> Controls were excluded if they had a family history of migraine or used over the counter/prescription pain medication for more than 5 days per month.

Each CM participant underwent 3 MRI scans: (1) immediately before their first SPG treatment, (2) 30 minutes after the initial treatment, and (3) 30 minutes after the last treatment of a series of 12 SPG blocks (twice per week). For the purposes of investigating the long term effect of a series of SPG treatment on neural networks, participants were scanned 30 minutes after the first treatment to account for any acute network connectivity changes. CM<sup>w/MOH</sup> participants were scanned at their baseline level of pain, at least 24 hours outside of their acute pain exacerbation period; any participant who came in within 24 hours of acute pain exacerbation was rescheduled.

**Clinical Parameters.**—All participants underwent vital sign evaluations including a neurological examination and completed a standardized questionnaire to ascertain clinical characteristics and demographic information (ie, age, sex, race, BMI, and educational level). The clinical characteristics included: (1) duration of migraine history, (2) duration of CM history, (3) family history of migraine, (4) current medications, (5) number of moderate to severe headache days per month, (6) location of migraine, (7) presence of aura, (8) headache-related disability as determined by Headache Impact Test (HIT-6<sup>®</sup>),<sup>16</sup> (9) depression as determined by Patient Health Questionnaire (PHQ-9),<sup>17</sup> (10) allodynia as measured by allodynia symptom checklist (ASC 12).<sup>18</sup>

**Standard Protocol Approvals, Registrations, and Participant Consent.**—The study protocol was approved by the institutional review board at University of South Carolina. Written informed consent was obtained from all participants.

**Transnasal SPG Block.**—In this study, all CM<sup>w/MOH</sup> participants received a series of 12 SPG blockade (twice per week for 6 weeks) using the Tx360<sup>®</sup> (Tian Medical Inc; Lombard, IL, USA) with 0.5% bupivacaine. This device uses a small, flexible, soft plastic catheter to advance below the middle turbinate just past the sphenopalatine foramen. The plastic tube can then be rotated laterally on a preset track and extended into the intranasal cavity. A total of 0.3 mL of 0.5% bupivacaine is administered into each nostril over the mucosa covering the SPG.<sup>6,7</sup> Dosing and anesthetic type was determined per device manufacturer's recommendations.

**MR Imaging Acquisition.**—All participants were scanned on a Siemens 3T scanner located at the McCausland Center for Brain Imaging (Columbia, SC). Some participants (n = 4) completed sets (before and after treatment) of scans prior to a system hardware (Trio to Prisma) upgrade; however, any variance due to this upgrade was controlled for in our analysis by adding this as a nuisance regressor variable to the general linear model using the Freedman-Lane approach.<sup>19</sup> Participants were instructed to keep their eyes closed, stay awake, relax, and think of "nothing in particular" during the resting state scan. All conditions and lighting

were consistent throughout the entire study for all participants.

The imaging parameters for the Trio (12 channel head/neck coil) system consisted of a 6 minute high-resolution T1 weighted magnetization-prepared rapid gradient echo (MP-RAGE) scan (repetition time [TR] = 2250 ms, echo time [TE] = 4.15 ms, 192 slices, 50% slice gap, flip angle = 9°, voxel size = 1.0 mm<sup>3</sup>, Field of View [FOV] = 256 mm<sup>2</sup>, iPAT factor of 2, and using a sagittal, ascending, single shot acquisition) and a 15 minute resting state functional imaging scan using a T2\* weighted BOLD contrast-sensitive sequence ([TR] = 1550 ms, [TE] = 34 ms, 42 slices, 20% slice gap, flip angle = 71°, voxel size = 2.5 mm<sup>3</sup>, FOV = 215 mm<sup>2</sup>, and using a transversal, interleaved acquisition).

The imaging parameters for the Prisma (20 channel head/neck coil [16/4]) system included an acquisition of 6-minute high resolution T1 weighted MP-RAGE scan (same parameters as Trio except that TE = 4.11 ms) and a 15-minute resting state functional imaging scan using a T2\* weighted BOLD contrast-sensitive sequence (TR = 1100 ms, TE = 35ms, 56 slices, 20% slice gap, flip angle = 72°, voxel size = 2.4 × 2.4 × 2.0 mm<sup>3</sup>, FOV = 216 mm<sup>2</sup>, and using a transversal, interleaved acquisition).

**MR Imaging Processing.**—Rs-fMRI preprocessing was completed using a combination of Statistical Parametric Mapping 12 software and custom Matlab scripts. The pipeline consisted of standard procedures including motion correction, coregistration, normalization, frequency filtering (0.01 to 0.1 Hz band-pass), and spatial smoothing (8 mm full width at half maximum). For each network, a connectivity atlas was constructed using spherical (15 mm diameter) regions of interest (ROIs) centered on the peak Montreal Neurological Institute (MNI) coordinates for the a priori networks of SN and EN.<sup>20</sup>

The SN<sup>20</sup> includes the bilateral dorsal anterior cingulate cortex (dACC), bilateral dorsolateral prefrontal cortex (dlPFC), left anterior PFC (aPFC), bilateral hypothalamus, bilateral orbital frontal insula (OFI), paracingulate cortex, bilateral extended amygdala (EA), bilateral supramarginal gyrus (SMG), left periaqueductal gray, bilateral supplementary motor area (SMA)/pre SMA,

bilateral ventral tegmental area/substantia nigra (VTA/SNPC), bilateral superior temporal, bilateral temporal pole, bilateral ventral striatum/pallidum (vSP), and right ventrolateral PFC (vlPFC). The CEN<sup>20</sup> consists of the bilateral anterior thalamus, bilateral dlPFC, bilateral dorsal PFC region of frontal eye fields (dPFC/FEF), bilateral vlPFC, dorsal medial PFC (dmPFC), right inferior frontal gyrus (IFG)/frontal operculum, right inferior temporal, bilateral lateral parietal, left OFI, bilateral dorsal caudate (dCaudate), and right ventromedial caudate (vmCaudate). The exact ROIs (and their MNI coordinates) can be found in our previous publication<sup>9,10</sup> and are illustrated in Figure 1.

**Statistical Analysis.**—To create a functional connectivity matrix for each participant, the following steps were taken using MATLAB. First, we extracted the BOLD time series from each ROI (node) within a network (defined a priori).<sup>20</sup> Then, for each network, a functional connectivity matrix was created by extracting the Fisher Z transformed Pearson's correlation coefficient (*r*) for each pair of ROIs. The intranetwork connectivity strength (Table 1) is defined as the correlation coefficient (fisher Z transformed Pearson *r* value) generated for each pair of nodes within the network investigated. The overall connectivity strength of a network was derived by averaging all NTNC within each network.

We investigated the intranetwork NTNC in the SN (n = 351) and CEN (n = 136). For each network, a 2-tailed, paired sample *t*-test was used to evaluate difference in NTNC when comparing baseline to 30 minutes after first treatment, and baseline to 30 minutes after the last treatment (at 6 weeks; "End of Treatment [EOT]"). Each statistical test employed a permutation method, using 10,000 permutations, to control for multiple comparisons (using MATLAB).<sup>21</sup> For each 9999 random permutations as well as the one actual ordering we logged the peak *t*-score for all regions (eg, maximum of 351 regions for SN). We then sorted these maximums and used the 500th most significant peak as our threshold to provide robust control for familywise error. These corrected *P* values of <.05 were considered significant for NTNC differences. No formal statistical test was

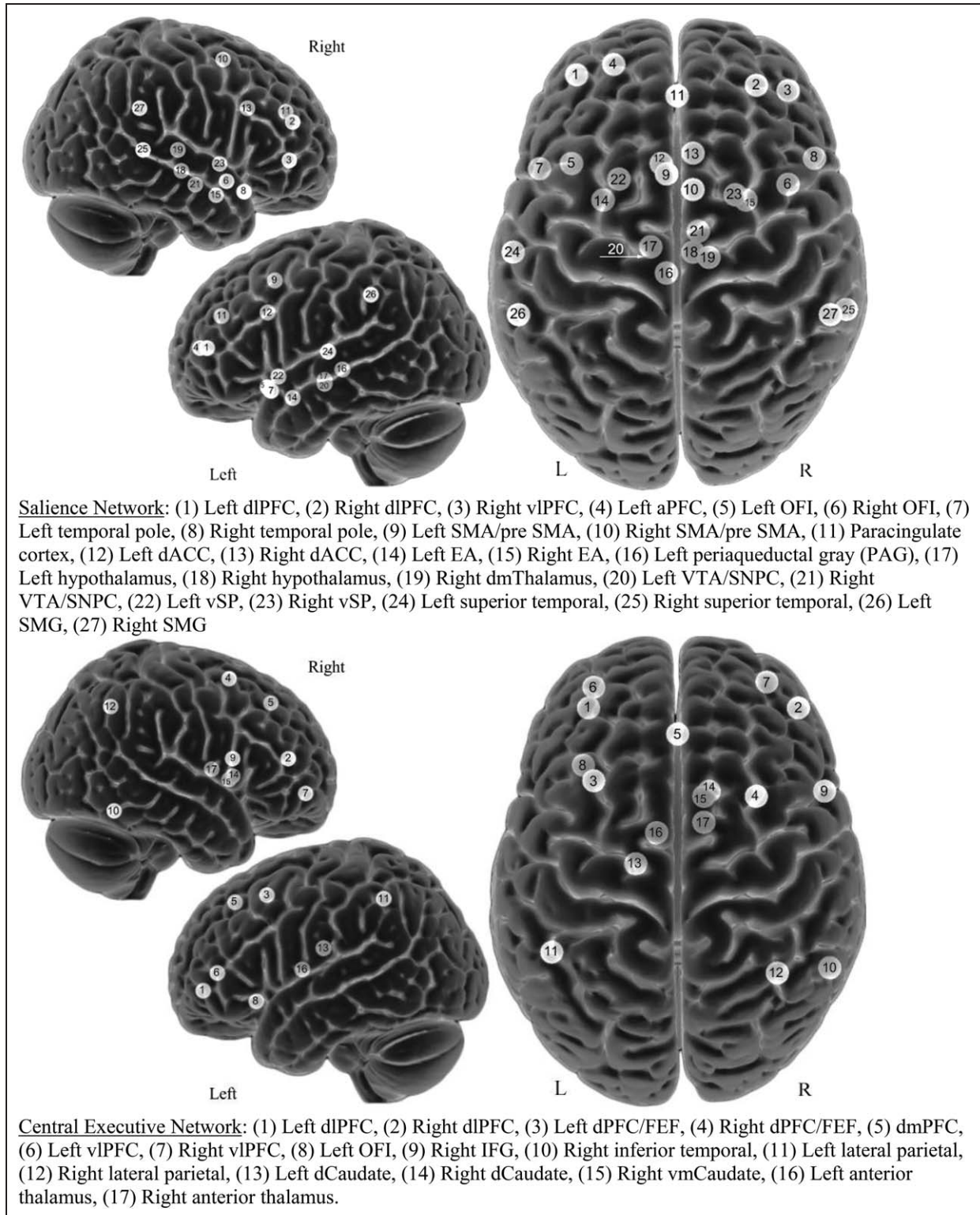


**Fig. 1.**—Axial and sagittal view of the salience (top) and central executive networks (bottom) as shown using the exact MNI coordinates. Images were made with “Surf Ice” (<https://www.nitrc.org/projects/surface/>). Node depth is illustrated by transparency with darker grey representing greater distance from the cortex.

Table 1.—Significantly Improved Intranetwork Nodal to Nodal Connectivity After Treatment

	Controls	Baseline	End of treatment	P-value
Saliency network				
Left aPFC × Left OFI	0.12 ± 0.23	0.03 ± 0.18	0.11 ± 0.21	.046
Left aPFC × Right OFI <sup>†</sup>	0.25 ± 0.32	0.15 ± 0.18	0.26 ± 0.28	.012
Left aPFC × Left vSP	0.21 ± 0.18	0.02 ± 0.19	0.14 ± 0.19	.022
Left aPFC × Right vSP <sup>†</sup>	0.26 ± 0.22	0.05 ± 0.17	0.22 ± 0.19	.021
Left aPFC × Right SMA/preSMA	0.37 ± 0.31	0.25 ± 0.25	0.32 ± 0.3	.038
Left aPFC × Right dlPFC	0.51 ± 0.23	0.43 ± 0.15	0.62 ± 0.2	.032
Left dlPFC × Right VTA/SNPC	0.05 ± 0.15	−0.1 ± 0.12	0.03 ± 0.17	.040
Right Temporal Pole × Right VTA/SNPC	0.09 ± 0.19	0.00 ± 0.23	0.08 ± 0.2	.020
Left Superior Temporal × Right SMG	0.11 ± 0.27	0.19 ± 0.33	0.13 ± 0.25	.030
Central executive network				
Left dlPFC × Left vlPFC	0.61 ± 0.27	0.6 ± 0.14	0.61 ± 0.23	.019
Left dlPFC × Right Anterior Thalamus <sup>†</sup>	0.28 ± 0.17	0.17 ± 0.11	0.27 ± 0.16	.027
Left dlPFC × Right vmCaudate	0.19 ± 0.15	0.15 ± 0.12	0.20 ± 0.17	.049
Left dlPFC × Right dPFC/FEF <sup>†</sup>	0.38 ± 0.24	0.2 ± 0.21	0.34 ± 0.23	.021
Left vlPFC × Right dPFC/FEF <sup>†</sup>	0.35 ± 0.24	0.24 ± 0.15	0.29 ± 0.18	.043
Left dPFC/FEF × Right Anterior Thalamus	0.21 ± 0.17	0.03 ± 0.17	0.18 ± 0.17	.028
Left dPFC/FEF × Right vmCaudate	0.16 ± 0.12	0.00 ± 0.14	0.04 ± 0.14	.011
Right dPFC/FEF × Right dCaudate	0.22 ± 0.14	0.01 ± 0.14	0.12 ± 0.18	.028

<sup>†</sup>Intranetwork connections that were also significantly different when comparing baseline to 30 minutes after the first treatment. Values represent mean ± standard deviation. The values listed in the “Controls” column are to illustrate what the “normal” connectivity strength is for the identified intranetwork connections (mean ± standard deviation of 10 control subjects). The *P* values listed are comparing the baseline to end of treatment within the SPG group (paired sample).

Abbreviations: aPFC, anterior PFC; dCaudate, dorsal caudate; dlPFC, dorsolateral prefrontal cortex; dPFC/FEF, dorsal PFC/frontal eye field; OFI, orbital frontal insula; PFC, prefrontal cortex; SMG, supramarginal gyrus; SMA, supplementary motor area; VTA/SNPC, ventral tegmental area/substantia nigra; vSP, ventral striatum/pallidum; vlPFC, ventrolateral PFC; vmCaudate, ventromedial caudate.

used to compare the CM data with the control data, as the connectivity data for the controls were only used to visually demonstrate the normalization of the CM group after the SPG series.

## RESULTS

**Participants.**—A total of 24 women (14 CM and 10 controls) were recruited between January 2015 and August 2016 from the University of South Carolina headache clinic (Columbia, SC). Four participants from the CM group were excluded due to the following reasons: motion artifact (*n* = 1), scanner error (*n* = 2), and unreported comorbid pain condition (*n* = 1). Among the 10 participants, 8 had bilateral headaches, and 2 had left sided headaches. Individual characteristics for the CM group are summarized in Table 2. The control (*n* = 10) participants were matched by age ( $41.9 \pm 11.5$ ) and BMI ( $28.6 \pm 5.7$ ).

**Behavioral and Clinical Data.**—Compared to baseline values, the number of moderate/severe headache days per month (*P* < .001), HIT-6 score (*P* < .001), PHQ-9 scored (*P* = .008) were all significantly improved at the EOT. Allodynia score was not significantly reduced at the EOT (*P* = .238). In addition to improved headache impact measurements, use of opioids (*P* = .001), NSAID (*P* = .0016), and triptans (*P* = .003) were also significantly reduced at EOT. All behavioral data are summarized in Table 2 and specific medication used per participant is summarized in Table 3.

**fMRI Data.**—When comparing baseline to EOT connectivity, several NTNC connections were significantly improved within the SN (*n* = 9) and CEN (*n* = 8) (Table 1, Fig. 2). Within the SN, improved connectivity was observed after treatment between the left aPFC to bilateral OFI and vSP, and contralateral SMA and dlPFC. Additionally, between right VTA/SNPC to

**Table 2.—Demographic and Clinical Features of Chronic Migraine With Medication Overuse Participants**

Demographics:				
<i>n</i>	10	BMI	28.5 ± 7.6	
Gender	10 females	Age	43.3 ± 13.1	
Race/ethnicity	8 Caucasian; 2 African American			
Headache characteristics		Baseline	End of treatment	<i>P</i> -value
Number moderate/severe headache days per month		21.1 ± 6.6	11.2 ± 6.5	<.001*
Allodynia score		6.4 ± 3.4	5.3 ± 4.5	.238
HIT-6 (headache impact test)		66.1 ± 2.6	60.2 ± 3.6	<.001*
PHQ-9 (patient health questionnaire)		12.1 ± 5.7	6.1 ± 3.6	.008*
Medication use (days/month)		Baseline	End of Treatment	<i>P</i> -value
Days of opioid use (n = 7)		19.7 ± 10.1	2.6 ± 2.8	.001*
Days of NSAIDs use (n = 7)		17.1 ± 10.2	6.3 ± 11.5	.006*
Days of triptan use (n = 8)		14.5 ± 7.3	6.5 ± 5.8	.003*
Headache history				
History of chronic migraine (years)		2.4 ± 1.2		
Family history (first degree)		n = 8 (1 unknown)		
History of migraine (years)		26.4 ± 12.0		

Values represent mean ± standard deviation.

\*Significant.

contralateral dIPFC and ipsilateral temporal pole. Lastly, a decrease in connectivity was observed between the left superior temporal and contralateral SMG; however, the trends suggest this still normalizes similar to the control data. Within the CEN, improved connectivity was observed between the left dIPFC to contralateral anterior thalamus, vmCaudate, dPFC/FEF, and ipsilateral vIPFC, as well as between the left

dPFC/FEF to contralateral anterior thalamus and vmCaudate. Lastly, between right dPFC/FEF to ipsilateral dCaudate and contralateral vIPFC. We did observe improvement in the overall the connectivity (averages of all NTNC in a network) of the CEN (Baseline 0.00 ± 0.08; 6 weeks 0.03 ± 0.09, *P* = .01), but not the SN (Baseline -0.01 ± 0.10; 6 weeks 0.01 ± 0.12, *P* = .26).

**Table 3.—Reduction in the Use of Acute Pain Medications for Each Participant**

Participants	Opioids or butalbital/month (Baseline, during treatment, % reduction)			NSAIDs/month (Baseline, during treatment, % reduction)			Triptans/month (Baseline, during treatment, % reduction)		
	01	30	6	80%	–	–	–	11	7
02	30	4	87%	10	0	100%	30	17	43%
03	–	–	–	30	30	0%	8	0	100%
04	30	0	100%	–	–	–	20	0	100%
05	18	6	67%	28	13	54%	11	5	55%
06	10	0	100%	21	0	100%	11	7	37%
07	12	0	100%	6	0	100%	10	4	60%
08	8	2	75%	5	1	80%	–	–	–
09	–	–	–	20	0	100%	–	–	–
10	–	–	–	–	–	–	15	12	20%

Medication use was calculated by how many days in a month (30 days) the medication was used. Baseline use was determined in a period of 30 days before treatment and during treatment use was determined by the last 30 days of their treatment period.

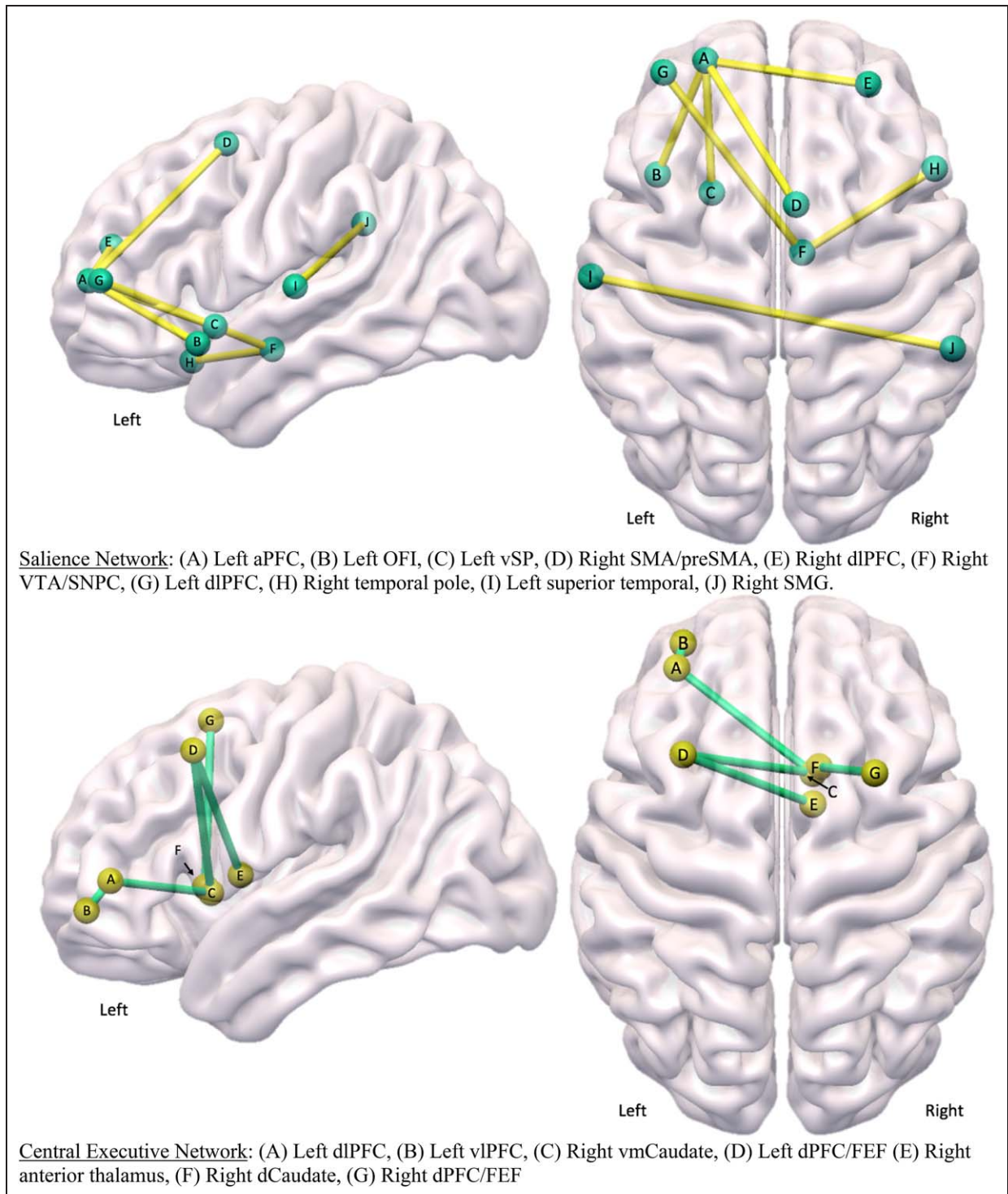


**Fig. 2.—Improved node to node intranetwork connectivity, unique to baseline vs end of treatment, within the salience network (top) and the central executive network (bottom) after a series of SPG blocks. [Color figure can be viewed at wileyonlinelibrary.com]**



## DISCUSSION

After recurrent parasympathetic inhibition via a series of SPG blocks, we have identified not only improved overall CEN connectivity, but also several intranetwork connections between regions of PFC (aPFC, dlPFC, vlPFC, and dPFC/FEF) and various limbic structures, as well as between different cortical regions. As CM is largely accompanied by pain and autonomic symptoms, variations in functional brain networks connectivity are thought to occur from the overwhelming need for the perception of pain and autonomic dysfunction. In normal pain modulation, increased activation of the aPFC, dlPFC, and vlPFC inhibit the painful stimuli from reaching the pain processing regions, contributing to an analgesic effect.<sup>22-24</sup> These key prefrontal regions, vital to the cognitive (top down pain modulation) aspect of pain processing and relevant saliency (bottom up filtration) of pain modulation, have been found to be dysregulated in CM<sup>w/MOH</sup> patients.<sup>9,10,25</sup> Interestingly, connectivity between many of these dysregulated regions in both networks exhibit a marked improvement after a series of SPG treatments.

**Saliency Network.**—Our result suggests that the function of the SN, regardless of increased or decreased connectivity (synchronization) at baseline in CM<sup>MOH</sup>, were partially restored to a normal state after treatment. Specifically, we noted near complete recovery of connectivity between the left aPFC, and various cortical and limbic regions (OFI, VTA/SNPC, and vSP) within SN. It is possible that recurrent SPG inhibition modified these connectivities, given the relative close proximity of SPG to aPFC and the importance of left PFC in parasympathetic function.<sup>26</sup> Interestingly, midbrain dopamine neurons (including VTA and SNPC) are the key regions of the reward network, and disruptions in these regions are implicated in overuse of pain medications.<sup>27,28</sup> Therefore, the improved synchronization between these regions may result in the decreased desire for taking acute pain medications, which is evident by the significant reduction in acute pain medication usage in our participants (Tables 2 and 3). Despite these subjectively near normalized NTNC, we did not observe improvement of overall SN connectivity. Clinically, this

may explain why the allodynia score was not significantly lower in our participants after treatment, given that this network connectivity is correlated with changes in allodynia score.<sup>9</sup> Our data suggest that repetitive SPG inhibition may help to reduce the saliency of pain by partially reversing the aberrant cortical and subcortical connectivity within the mesocorticolimbic system in these patients.

**Central Executive Network.**—Within the CEN, improved connectivity was observed in overall connectivity strength and between regions of the PFC and cortico-thalamic-striatal regions. Cognitive control in pain modulation is diverted to “pain-reduction-related processes” in CM.<sup>29</sup> As many of these PFC regions within the CEN are also involved in pain modulation pathways, it is likely that these disruptions in the CEN are related to constant “hijacking” of cognitive resources. The improved connectivity of several frontal cortex regions were demonstrated in our participants, and may be reflective of a lessening of burden on these cognitive resources. Taken together, these findings further support the hypothesis that recurrent parasympathetic inhibition is associated with improved functional connectivity in brain regions critical to pain processing in CM<sup>w/MOH</sup>.

**Left Prefrontal Cortex.**—Across both networks we found that the majority of the PFC regions that recovered after treatment are in the left hemisphere. Locations of the headaches in our patients do not seem to have any impact on this, as 80% of them had bilateral headaches. The autonomic control in the central nervous system is maintained through homeostatic balance between the left (parasympathetic) and right PFC (sympathetic).<sup>26</sup> As SPG blockade is most likely to affect parasympathetic outflow, this may explain why left PFC regions appear to improve more after treatment. We postulate that repetitive parasympathetic inhibition via SPG may restore the homeostatic balance by predominantly improving parasympathetic tone in the left PFC.

**Limitations.**—We do acknowledge there are limitations of this pilot study. First, the sample size is small; however, we were able to reach sufficient statistical power using a longitudinal, within the group

comparison design. Future studies would benefit from increased sample size, and scanning healthy controls at the same time point intervals to control for any longitudinal brain connectivity changes. Second, it is possible that the improved connectivity may be partially related to the placebo effect. To control for this, we examined common improvements, seen in the analysis of baseline vs 30 minutes after first treatment and baseline vs EOT, to highlight any similarly improved nodes. These nodes that showed improved connectivity have been previously implicated in placebo analgesia<sup>30</sup> and may be associated with immediate pain reduction or “anticipation of pain relief.” Ideally, a double blinded placebo controlled methodology could have been employed. However, as a pilot study, the purpose was not to evaluate the efficacy of SPG in CM<sup>w/MOH</sup>, but rather to investigate the longitudinal intrinsic functional brain network connectivity changes associated with this treatment.

Another possible confounder is the reduction of acute pain medication usage which occurred in all of our patients, likely due to reduced headache frequency (Table 3). For ethical reasons, use of acute pain medication could not be maintained. However, given significant reduction of migraine days in these patients, a possible explanation is that successful detoxification with the treatment modified the risk factor for CM<sup>w/MOH</sup>. Despite this, we still think a larger cohort study to investigate the confounding effects of acute medications on resting state connectivity using a multivariate linear regression model may be helpful to address this issue. Additionally, we cannot be certain that our findings are a *consequence* of SPG inhibition or if they are *causal*, as we are unable to determine if these changes in connectivity are due to reduced headache/migraine or if is a response to a general reduction of chronic pain. This question maybe better answered using a cohort group of another chronic pain disorder. Currently, there is no technique to definitively confirm that only SPG was targeted by the local anesthesia using intranasal approach, other nearby structures such as maxillary branch of trigeminal nerve may have been affected by the treatment.

## CONCLUSION

Despite incomplete normalization of the functional brain networks, our results suggest that recurrent parasympathetic inhibition via a series of SPG blocks is associated with long term neuromodulatory effect in CM<sup>w/MOH</sup>. We postulate that repetitive SPG inhibition may modulate the activity of various neuropeptides within the ganglion, resulting in improved resting state intrinsic functional connectivity, especially the left PFC, likely through decreased parasympathetic outflow to cranial and meningeal vessels. Furthermore, it may modulate resting state functional connectivity in mesocorticolimbic regions, likely through the connection between SPG to SSN.<sup>31</sup> These bidirectional effects originating from the recurrent SPG inhibition extracranially may subsequently lead to partial restoration of the affected connectivity changes associated with CM<sup>w/MOH</sup>. Future study with a large sample size is needed to further unravel the neurobiological basis underlying the role of SPG in CM<sup>w/MOH</sup>.

## STATEMENT OF AUTHORSHIP

### Category 1

#### (a) Conception and Design

X. Michelle Androulakis, Kaitlin Krebs

#### (b) Acquisition of Data

X. Michelle Androulakis, Kaitlin Krebs

#### (c) Analysis and Interpretation of Data

X. Michelle Androulakis, Kaitlin Krebs, Chris Rorden

### Category 2

#### (a) Drafting the Manuscript

X. Michelle Androulakis, Kaitlin Krebs

#### (b) Revising It for Intellectual Content

X. Michelle Androulakis, Kaitlin Krebs, Chris Rorden

### Category 3

#### (a) Final Approval of the Completed Manuscript

X. Michelle Androulakis, Kaitlin Krebs, Chris Rorden

## REFERENCES

1. Khan S, Schoenen J, Ashina M. Sphenopalatine ganglion neuromodulation in migraine: What is the rationale? *Cephalalgia*. 2014;34:382-391.
2. Robbins MS, Robertson CE, Kaplan E, et al. The sphenopalatine ganglion: Anatomy, pathophysiology, and therapeutic targeting in headache. *Headache*. 2016;56:240-258.
3. Goadsby PJ, Lipton RB, Ferrari MD. Migraine—current understanding and treatment. *N Engl J Med*. 2002;346:257-270.
4. Moskowitz MA. Basic mechanisms in vascular headache. *Neurol Clin*. 1990;8:801-815.
5. Maizels M, Aurora S, Heinricher M. Beyond neurovascular: Migraine as a dysfunctional neurolimbic pain network. *Headache*. 2012;52:1553-1565.
6. Cady R, Saper J, Dexter K, Manley HR. A double-blind, placebo-controlled study of repetitive transnasal sphenopalatine ganglion blockade with Tx360<sup>®</sup> as acute treatment for chronic migraine. *Headache*. 2015;55:101-116.
7. Cady RK, Saper J, Dexter K, Cady RJ, Manley HR. Long-term efficacy of a double-blind, placebo-controlled, randomized study for repetitive sphenopalatine blockade with bupivacaine vs saline with the Tx360<sup>®</sup> device for treatment of chronic migraine. *Headache*. 2015;55:529-542.
8. Yarnitsky D, Goor-aryeh I, Bajwa Z, et al. Possible parasympathetic contributions to peripheral and central sensitization during migraine. *Headache*. 2003;43:704-715.
9. Androulakis XM, Krebs K, Peterlin BL, et al. Modulation of intrinsic resting-state fMRI networks in women with chronic migraine. *Neurology*. 2017;10-212.
10. Androulakis XM, Rorden C, Peterlin BL, Krebs KA. Modulation of salience network intranetwork resting state functional connectivity in women with chronic migraine. *Cephalalgia*. 2018; Accepted.
11. Ferraro S, Grazi L, Mandelli ML, et al. Pain processing in medication overuse headache: A functional magnetic resonance imaging (fMRI) study. *Pain Med*. 2012;13:255-262.
12. Cahill CM, Cook C, Pickens S. Migraine and reward system—or is it aversive? *Curr Pain Headache Rep*. 2014;18:410.
13. Koob GF, Volkow ND. Neurocircuitry of addiction. *Neuropsychopharmacology*. 2010;35:217-238.
14. Jasinska AJ, Stein EA, Kaiser J, Naumer MJ, Yalachkov Y. Factors modulating neural reactivity to drug cues in addiction: A survey of human neuroimaging studies. *Neurosci Biobehav Rev*. 2014;38:1-6.
15. The International Classification of Headache Disorders, 3rd edition (beta version). Headache Classification Committee of the International Headache Society (IHS). *Cephalalgia*. 2013;33(9):629-808.
16. Shin HE, Park JW, Kim YI, Lee KS. Headache Impact Test-6 (HIT-6) scores for migraine patients: Their relation to disability as measured from a headache diary. *J Clin Neurol*. 2008;4:158-163.
17. Seo JG, Park SP. Validation of the Patient Health Questionnaire-9 (PHQ-9) and PHQ-2 in patients with migraine. *J Headache Pain*. 2015;16:65.
18. Lipton RB, Bigal ME, Ashina S, et al. Cutaneous allodynia in the migraine population. *Ann Neurol*. 2008;63:148-158.
19. Freedman D, Lane D. A nonstochastic interpretation of reported significance levels. *J Bus Econ Stat*. 1983;1:292-298.
20. Seeley WW, Menon V, Schatzberg AF, et al. Dissociable intrinsic connectivity networks for salience processing and executive control. *J Neurosci*. 2007;27:2349-2356.
21. Winkler AM, Ridgway GR, Webster MA, Smith SM, Nichols TE. Permutation inference for the general linear model. *Neuroimage*. 2014;92:381-397.
22. Lorenz J, Minoshima S, Casey KL. Keeping pain out of mind: The role of the dorsolateral prefrontal cortex in pain modulation. *Brain*. 2003;126:1079-1091.
23. Salomons TV, Johnstone T, Backonja MM, Shackman AJ, Davidson RJ. Individual differences in the effects of perceived controllability on pain perception: Critical role of the prefrontal cortex. *J Cogn Neurosci*. 2007;19:993-1003.
24. Wiech K, Kalisch R, Weiskopf N, et al. Anterolateral prefrontal cortex mediates the analgesic effect of expected and perceived control over pain. *J Neurosci*. 2006;26:11501-11509.
25. Bingel U, Tracey I. Imaging CNS modulation of pain in humans. *Physiology*. 2008;23:371-380.
26. Hilz MJ, Dütsch M, Perrine K, et al. Hemispheric influence on autonomic modulation and baroreflex sensitivity. *Ann Neurol*. 2001;49:575-584.
27. Kuhnen CM, Knutson B. The neural basis of financial risk taking. *Neuron*. 2005;47:763-770.
28. Corlett PR, Aitken MR, Dickinson A, et al. Prediction error during retrospective reevaluation of

- causal associations in humans: fMRI evidence in favor of an associative model of learning. *Neuron*. 2004;44:877-888.
29. Mathur VA, Khan SA, Keaser ML, et al. Altered cognition-related brain activity and interactions with acute pain in migraine. *Neuroimage Clin*. 2015;7:347-358.
  30. Wager TD, Rilling JK, Smith EE, et al. Placebo-induced changes in FMRI in the anticipation and experience of pain. *Science*. 2004;303:1162-1167.
  31. Akerman S, Holland PR, Goadsby PJ. Diencephalic and brainstem mechanisms in migraine. *Nat Rev Neurosci*. 2011;12:570-584.